JACS
JOURNAL OF THE AMERICAN CHEMICAL SOCIETY
Communication
pubs.acs.org/JACS

# Photoconductive Cathode Interlayer for Highly Efficient Inverted Polymer Solar Cells

Li Nian,[†] Wenqiang Zhang,[†] Na Zhu,[†] Linlin Liu,[†] Zengqi Xie,*[,†] Hongbin Wu,[†] Frank Würthner,[‡] and Yuguang Ma*[,†]

[†]Institute of Polymer Optoelectronic Materials and Devices, State Key Laboratory of Luminescent Materials and Devices, South China University of Technology, Guangzhou 510640, China

[‡]Institut für Organische Chemie & Center for Nanosystems Chemistry, Universität Würzburg, Am Hubland, 97074 Würzburg, Germany

Supporting Information

**ABSTRACT:** A highly photoconductive cathode interlayer was achieved by doping a 1 wt % light absorber, such as perylene bisimide, into a ZnO thin film, which absorbs a very small amount of light but shows highly increased conductivity of $4.50 \times 10^{-3}$ S/m under sunlight. Photovoltaic devices based on this kind of photoactive cathode interlayer exhibit significantly improved device performance, which is rather insensitive to the thickness of the cathode interlayer over a broad range. Moreover, a power conversion efficiency as high as 10.5% was obtained by incorporation of our photoconductive cathode interlayer with the PTB7-Th:$PC_{71}BM$ active layer, which is one of the best results for single-junction polymer solar cells.

Polymer solar cells (PSCs) have drawn much research interest in the past decades as one of the promising candidates of a clean energy source for potentially low cost and fast roll-to-roll production.[1] Inverted polymer solar cells (i-PSCs) as the counterpart of the conventional polymer solar cells (c-PSCs) possess major advantages of enhanced device performance as well as increased stability.[2] With the rapid progress in recent years, power conversion efficiency (PCE) over 10% has been achieved in single-junction i-PSCs.[3] Rapid advancement of PCE benefits from the development of novel electron-donating materials and interfacial engineering.[4] In particular, the cathode interlayer between the active layer and conductive ITO electrode plays a key role in the performance of i-PSCs due to their fundamental importance to the electron extraction process.[5] In the most recent years, polymeric surfactants like conjugated poly[(9,9-bis(3-(*N*,*N*-dimethylamino)propyl)-2,7-fluorene)-*alt*-2,7-(9,9-dioctylfluorene)] and nonconjugated ethoxylated polyethyleneimine (PEIE) were successfully applied as the cathode interlayers, yielding highly efficient inverted PSCs.[6] Typically, the thickness of such interlayer is less than 10 nm, and the device performance is very sensitive to the thickness of this interlayer for the low conductivity of this kind of surfactant. Massive production of such a thin film is quite difficult and may restrict its wide application especially in printed PSCs in the future. To realize fully printed PSCs, more and more attention has been paid on the development of highly conductive and thickness-insensitive interlayer materials. For example, Jen and co-workers reported a highly conductive PEIE-doped fullerene derivative as a cathode interlayer, which resulted in high device performance even if the thickness of the interlayer was increased to 30−50 nm.[7] Other examples are based on self-assembled perylene bisimides and conjugated metallopolymers.[8]

Photoconductivity is an optical and electrical phenomenon in which a material becomes more electrically conductive due to the absorption of light.[9] Especially, organic−inorganic hybrid photoconductive materials have attracted much attention because they can take advantage of inherent features of both organic and inorganic materials simultaneously, that is, large extinction coefficients of organic semiconductors over a wide wavelength range and fast electron transport efficiency in inorganic semiconductors.[10] It was found that charge transfer rates from excited organic molecules to inorganic materials can be remarkably accelerated upon illumination when they are chemically attached.[11] For example, zinc oxide (ZnO), a typical well-established inorganic n-type semiconductor, hybridized with organic semiconductors shows promise for application in hybrid photovoltaic and photoconduction.[12] In this contribution, we report a highly photoconductive sol−gel-derived ZnO cathode interlayer by doping a very small amount of light absorber (i.e., PBI-H as shown in Chart 1)[13] as an example in the thin film. By using the photoactive ZnO:PBI-H film as the cathode interlayer atop the ITO electrode, we fabricated i-PSCs based on the classical polymer thieno[3,4-*b*]thiophene/benzodithiophene (PTB7):[6,6]-phenyl $C_{71}$-butyric acid methyl ester ($PC_{71}BM$) system (Chart 1 and Scheme 1) and achieved over 20% enhancement in PCE compared with the device using

**Chart 1. Chemical Structures of PBI-H, PTB7, PTB7-Th, and $PC_{71}BM$**

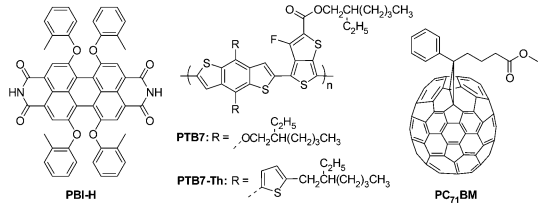


**Received:** February 28, 2015
**Published:** May 28, 2015




DOI: 10.1021/jacs.5b02168
*J. Am. Chem. Soc.* 2015, 137, 6995−6998

**Scheme 1. Device Configuration Investigated in This Work**[a]

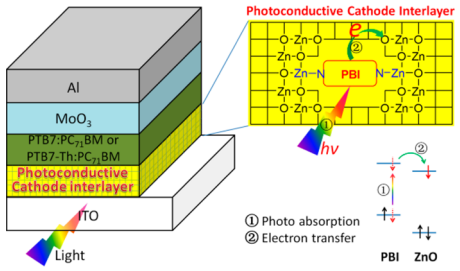


[a]Cathode interlayer indicates PBI-H-doped ZnO (ZnO:PBI-H). PBI-H molecules are chemically bound to ZnO, which accelerates electron transfer between them upon illumination, resulting in high photoconductivity.

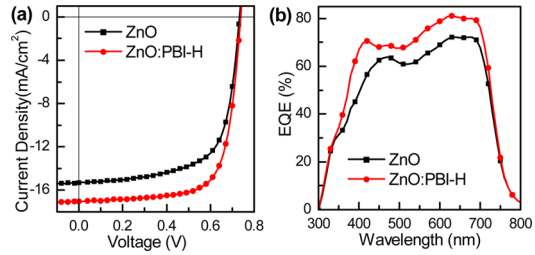


**Figure 1.** (a) $J-V$ characteristics of the i-PSCs under 1000 W/m$^2$ AM 1.5G illumination. (b) EQE curves. Device configurations are ITO/ZnO(30 nm) or ZnO:PBI-H(30 nm)/PTB7:$PC_{71}BM$ (100 nm)/$MoO_3$ (10 nm)/Al (100 nm).

pure ZnO as the cathode interlayer (from 7.42 to 9.01%). In addition, the device with the active layer based on a more efficient narrow band gap semiconducting polymer PTB7-Th[4e] gives a PCE as high as 10.5%, which is one of the best results for single-junction PSCs. For the high photoconductivity of this cathode interlayer, the high device performance is insensitive to its thickness over a broad range of 30−60 nm.

Sol−gel-derived ZnO films were prepared according to Heeger et al., using zinc acetate in 2-methoxyethanol:2-aminoethanol as a precursor solution by spin-coating followed by thermal treatment at 200 °C for 60 min.[14] Films of ZnO:PBI-H (at a weight ratio of 100:1) were derived by directly dissolving PBI-H into the precursor solution of ZnO for spin-coating, and they were also treated under the same conditions as above. As reported before, PBI-H is soluble in THF.[13] In contrast, the film of ZnO:PBI-H in THF, even if soaked for a long time, does not release PBI-H, while a ZnO film doped with PBI-$C_3H_7$ (see Supporting Information for the chemical structure) released the dye molecules immediately (Figure S1). Considering the difference of the chemical structures between PBI-H and PBI-$C_3H_7$, we proposed that PBI-H molecules might form a N−Zn bond with ZnO (Scheme 1) during the thermal treatment process according to a recent report.[15] To confirm the existence of this N−Zn bond, X-ray photoelectron spectroscopy was used to investigate the hybrid of ZnO and PBI-H using both individual components as the references. As illustrated in Figure S2, the slight peak position shift of N 1s for the hybrid toward lower bonding energy (BE) values compared to that of PBI-H (from 400.32 to 398.62 eV) indicates the interaction between ZnO and PBI-H through the N−Zn bond, and auxiliary evidence is given by the peak shift of Zn 2p for the hybrid to higher BE relative to that of ZnO (from 1020.82 to 1023.17 eV). This result is consistent with the previous finding in a naphthalene bisimide system, in which N−Zn formed at 140 °C.[15]

Nanoparticle-like morphology of the ZnO:PBI-H film with a small surface roughness (rms = 0.913 nm) was observed by atomic force microscopy (Figure S3). The smooth and robust thin film of ZnO:PBI-H (100:1 w/w ratio) was used as cathode interlayer for the fabrication of i-PSCs with a device configuration. As a reference, devices were also fabricated with ZnO as the cathode interlayer. Current density−voltage ($J-V$) characteristics of the inverted cells and the corresponding external quantum efficiency (EQE) are given in Figure 1; the extracted device performance metrics are given in Table 1. The device with a ZnO:PBI-H cathode interlayer exhibited a PCE of 9.01% with a $V_{oc}$ of 0.753 V, a $J_{sc}$ of 17.18 mA cm$^{-2}$, and a FF of 70.42%, which is significantly higher than the value obtained from the reference device using pure ZnO as the cathode interlayer that showed typical PCE of 7.42% ($V_{oc}$ of 0.732 V, $J_{sc}$ of 15.32 mA cm$^{-2}$, and FF of 67.25%) in accordance with reported values.[16] A significant positive effect of the ZnO:PBI-H-based device is that all $V_{oc}$, $J_{sc}$, and FF are simultaneously enhanced relative to the devices based on pure ZnO. The higher $V_{oc}$ of a ZnO:PBI-H-based device was related to the more favorable work function (WF) of the modified cathode that matches the lowest unoccupied molecular orbital (LUMO) of the $PC_{71}BM$, which will be discussed below. We attributed the higher $J_{sc}$ and FF to the improved charge selectivity at the cathode interface and charge transport ability of the cathode interlayer, as indicated by the significantly reduced dark current under reversed bias and enhanced dark current under forward bias in the dark $J-V$ curves of the corresponding devices (Figure S4). Indeed, the ZnO:PBI-H-based device showed greater than 30-fold improvement in rectification ratio relative to that of the pure ZnO-based device (from 0.6k for to 20k) at ±2 V. In addition, the internal quantum efficiency of the ZnO:PBI-H-based device was increased (Figure S5). It should be noted that the doping concentration of PBI-H was as low as 1 wt %, and the transparency of this interlayer was only slightly decreased by 1−2% in the range of 525−610 nm compared to the ZnO thin film (Figure S6); however, the PBI-H molecules contributed a lot to the performance of this interlayer, such as enhanced electron extraction and transport properties.

To understand the effect of doped PBI-H on the electron transport properties of the interlayers, electron-only devices comprising the ZnO:PBI-H and ZnO interlayers were fabricated with two device configurations. One is ITO/Al/interlayer/Ca/Al, which is used to test the electron transport properties of the interlayer (Figure 2a); the other one is ITO/Al/interlayer/PTB7:$PC_{71}BM$/Ca/Al, which is used to test the electron transport properties of the whole devices (Figure 2b). Electron mobility of the interlayer increased from $5.10 \times 10^{-4}$ for ZnO to $2.02 \times 10^{-3}$ cm$^2$ V$^{-1}$ s$^{-1}$ for ZnO:PBI-H. Note that the PBI-H-doped ZnO interlayer showed 4-fold enhancement of electron mobility compared with that of the ZnO interlayer, which is different from the previous reports where organic materials such as PVP, PEO, PEG, and PFEP-doped ZnO showed almost unchanged or even decreased electron transport properties.[17] Increased electron mobility in our doping system is quite similar to the recent report of a fullerene-derivative-doped ZnO.[3b,4e] Electron transport properties of the whole devices obtained from the second device configuration showed the same tendency that the apparent electron mobility of the whole device was increased from $5.11 \times 10^{-4}$ cm$^2$ V$^{-1}$ s$^{-1}$ (ZnO-based) to $3.96 \times 10^{-3}$ cm$^2$ V$^{-1}$ s$^{-1}$ (ZnO:PBI-H-based) (Figure 2b). These results are consistent with the higher FF value and the enhanced dark


DOI: 10.1021/jacs.5b02168
J. Am. Chem. Soc. 2015, 137, 6995−6998

**Table 1. Device Performance under 1000 W/m$^2$ AM Illumination**[a]

| device configuration | $V_{oc}$ (V) | $J_{sc}$ (mA/cm$^2$) | FF (%) | PCE (%)[b] | $R_s$ ($\Omega$ cm$^2$)[c] |
|---|---|---|---|---|---|
| ITO/ZnO/PTB7:$PC_{71}BM$/$MoO_3$/Al | 0.732 ± 0.004 | 15.32 ± 0.22 | 67.25 ± 0.11 | 7.42 ± 0.11(7.58) | 6.12 |
| ITO/ZnO:PBI-H/PTB7:$PC_{71}BM$/$MoO_3$/Al | 0.753 ± 0.005 | 17.18 ± 0.11 | 70.42 ± 0.12 | 9.01 ± 0.05(9.09) | 3.63 |
| ITO/ZnO/PTB7-Th:$PC_{71}BM$/$MoO_3$/Al | 0.788 ± 0.005 | 15.52 ± 0.27 | 67.86 ± 0.22 | 8.31 ± 0.13 (8.45) | 5.86 |
| ITO/ZnO:PBI-H/PTB7-Th:$PC_{71}BM$/$MoO_3$ /Al | 0.815 ± 0.005 | 17.54 ± 0.12 | 72.76 ± 0.14 | 10.48 ± 0.11 (10.59) | 3.05 |

[a]Data from 15 independent devices. [b]Maximum PCEs in brackets. [c]Series resistance ($R_s$) deduced from the $J-V$ curves of the best devices.

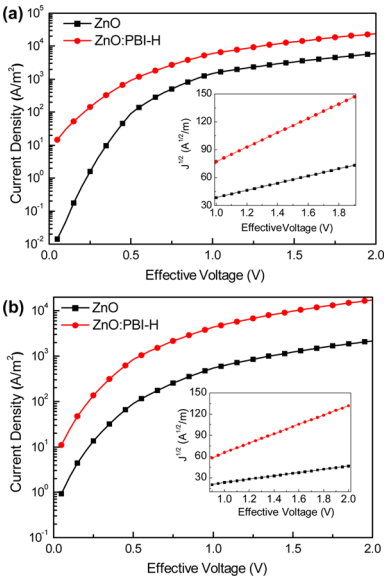


**Figure 2.** $J-V$ curves of the electron-only devices for (a) ITO/Al/interlayer (90 nm)/Ca/Al and (b) ITO/Al/interlayer (30 nm)/PTB7:$PC_{71}BM$/Ca/Al, in which the interlayer indicates ZnO or ZnO:PBI-H. The insets are $J^{1/2} \sim V$ characteristics of the electron-only devices.

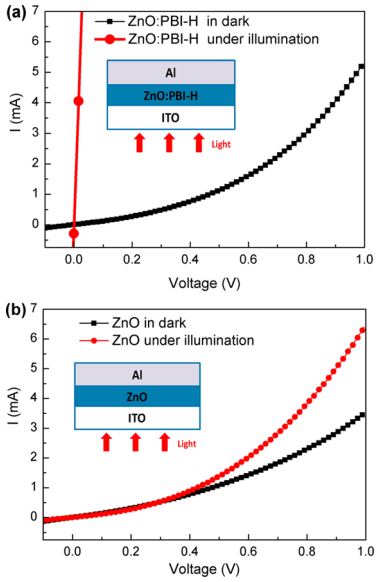


**Figure 3.** $I-V$ curves of the devices for (a) ITO/ZnO:PBI-H (90 nm)/Al and (b) ITO/ZnO (90 nm)/Al in the dark and under 1000 W/m$^2$ AM 1.5G illumination.

current under forward bias in the dark $J-V$ curves for the ZnO:PBI-H-based devices (Figure S4).

In addition, the ZnO:PBI-H film displayed distinct $I-V$ features in dark and under AM 1.5G 1000 W/m$^2$ illumination (ITO/ZnO:PBI-H/Al), as shown in Figure 3a. The device showed diode behavior with low current in the dark, whereas the $I-V$ curve became linear in relation to the high current under illumination (the current is increased by 50-fold at 1 V, Figure S7). In contrast, the reference device based on ZnO with the ITO/ZnO/Al configuration showed diode behavior with a low current in the dark and under illumination (Figure 3b). The $I-V$ curve transition implied that the ZnO:PBI-H film changed from semiconductor in the dark to conductor under illumination with the electrical conductivity determined to be ~$4.50 \times 10^{-3}$ S/m. High photoconductivity can be understood in terms of the photoinduced electron transfer from PBI-H to ZnO (Scheme 1), which largely increases the electron concentration on the conduction band (CB) of ZnO. Both increased electron mobility and electron concentration contributed to the high conductivity of ZnO:PBI-H film under light irradiation. Noticeably, this highly photoconductive interlayer is favorable for suppressing charge recombination and facilitating electron extraction for PSCs, as demonstrated in a conductive fullerene electron transport layer system.[7,18]

To find the reason for the increased $V_{oc}$ from 0.732 V (ZnO-based devices) to 0.753 V (ZnO:PBI-H-based devices), ultraviolet photoelectron spectroscopy was used to probe the electronic properties of the cathodes, including ZnO and ZnO:PBI-H-modified ITO (Figure S10 and Table S1). The WF of pure ZnO-modified ITO showed a value of ~4.2 eV, and it was decreased significantly to ~3.8 eV for the ZnO:PBI-H-modified ITO. The relatively lower WF of the ZnO:PBI-H indicates more population of electrons on the CB of ZnO under the measurement conditions. These data are consistent with the observed $V_{oc}$ values in different i-PSCs based on these interlayers. Moreover, the low WF value of ZnO:PBI-H-modified ITO allows ohmic contact to form with the $PC_{71}BM$ acceptor, which increases the built-in field, benefits to the enhanced charge extraction efficiency and the decreased recombination losses. This WF decreasing phenomenon is novel and cannot be explained by the most widely used interfacial dipole model.[5a]

As illustrated in Scheme 1, the energy level alignment between ZnO and the light absorber is essential for the photoinduced electron transfer process. In experiment, we also used porphyrin and tetrachlorinated perylene bisimide as the dopants; the former possesses a LUMO level higher than that of ZnO, and the latter has a relatively lower LUMO level than ZnO. The results indicate that the doping of porphyrin in ZnO enhanced the device performance, while the doping of tetrachlorinated perylene bisimide showed almost no effect, which clearly indicates the important role of the photoconductivity on the interlayer performance (Figure S11 and Table S2). To test the applicability of our photoconductive interlayer in various active layers in the devices, we fabricated i-PSCs using a more efficient narrow band gap semiconducting polymer, PTB7-Th, as the electron-donating polymer (Figure S12 and Table 1). The devices showed extremely high $PCE_{max}$ of 10.59% ($V_{oc}$ of 0.821 V, $J_{sc}$ of 17.69 mA cm$^{-2}$, and FF of 72.92%), which is also much


DOI: 10.1021/jacs.5b02168
J. Am. Chem. Soc. 2015, 137, 6995−6998

higher than that of the device with the same active layer but undoped ZnO cathode interlayer ($PCE_{max}$ = 8.45%).

Finally, a series of i-PSCs based on varied thickness of ZnO:PBI-H films were fabricated to evaluate the effect of ZnO:PBI-H thickness on device performance. PCE values of the devices are presented in Figure 4. It was shown that the device

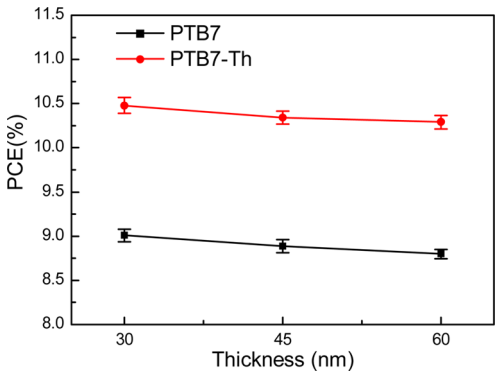


**Figure 4.** Effects of the thickness of the ZnO:PBI-H cathode interlayer on device performance. Device configuration: ITO/ZnO:PBI-H (*x* nm)/PTB7 or PTB7-Th:$PC_{71}BM$ (100 nm)/$MoO_3$ (10 nm)/Al (100 nm). Average values of seven cells with standard deviation.

performance is rather insensitive to the thickness of the ZnO:PBI-H layer. Even when the thickness reaches ~60 nm, the variety of the PCE value is less than 2.5%, which is attributed to the high photoconductivity of the ZnO:PBI-H films.

In conclusion, we have successfully demonstrated a great enhancement in PCE of i-PSCs by a photoconductive cathode interlayer prepared by doping ZnO with a light absorber. The very small amount of absorbed light gave a significant improvement in the conductivity of the ZnO:PBI-H films of $4.50 \times 10^{-3}$ S/m. Moreover, the PBI-H doping offered other great properties, including robust thin film, high electron mobility, and effective WF modification of the ZnO film. The i-PSCs based on the ZnO:PBI-H interlayer exhibited PCE values of 10.5% for PTB7-Th:$PC_{71}BM$ system. The photoconductive cathode interlayer may be achieved by doping various organic dyes into ZnO, which is quite useful for the development of novel thickness-insensitive cathode interlayers. The photodoping concept is also applicable in other organic electronic devices like OLEDs and photodetectors, and the work is ongoing in our lab.

## ■ ASSOCIATED CONTENT

### Supporting Information

Experimental details and characterization data. The Supporting Information is available free of charge on the ACS Publications website at DOI: 10.1021/jacs.5b02168.

## ■ AUTHOR INFORMATION

### Corresponding Authors

*msxiez@scut.edu.cn
*ygma@scut.edu.cn

### Notes

The authors declare no competing financial interest.

## ■ ACKNOWLEDGMENTS

We thank the financial support from the National Basic Research Program of China (973 Program) (2014CB643504, 2013CB834705), Natural Science Foundation of China (51373054, 51303057, 51473052, 21334002), and Introduced Innovative R&D Team of Guangdong (201101C0105067115).

## ■ REFERENCES

(1) (a) Yu, G.; Gao, J.; Hummelen, J. C.; Wudl, F.; Heeger, A. J. *Science* **1995**, *270*, 1789. (b) Beaujuge, P. M.; Fréchet, J. M. J. *J. Am. Chem. Soc.* **2011**, *133*, 20009. (c) Dou, L.; You, J.; Yang, J.; Chen, C.-C.; He, Y.; Murase, S.; Moriarty, T.; Emery, K.; Li, G.; Yang, Y. *Nat. Photonics* **2012**, *6*, 180.

(2) (a) Hsieh, C.-H.; Cheng, Y.-J.; Li, P.-J.; Chen, C.-H.; Dubosc, M.; Liang, R.-M.; Hsu, C.-S. *J. Am. Chem. Soc.* **2010**, *132*, 4887. (b) Dou, L.; Gao, J.; Richard, E.; You, J.; Chen, C.-C.; Cha, K. C.; He, Y.; Li, G.; Yang, Y. *J. Am. Chem. Soc.* **2012**, *134*, 10071.

(3) (a) Liu, Y.; Zhao, J.; Li, Z.; Mu, C.; Ma, W.; Hu, H.; Jiang, K.; Lin, H.; Ade, H.; Yan, H. *Nat. Commun.* **2014**, *5*, 5293. (b) Liao, S.-H.; Jhuo, H.-J.; Yeh, P.-N.; Cheng, Y.-S.; Li, Y.-L.; Lee, Y.-H.; Sharma, S.; Chen, S.-A. *Sci. Rep.* **2014**, *4*, 6813.

(4) (a) Song, C. K.; Luck, K. A.; Zhou, N.; Zeng, L.; Heitzer, H. M.; Manley, E. F.; Goldman, S.; Chen, L. X.; Ratner, M. A.; Bedzyk, M. J.; Chang, R. P. H.; Hersam, M. C.; Marks, T. J. *J. Am. Chem. Soc.* **2014**, *136*, 17762. (b) Wang, M.; Wang, H.; Yokoyama, T.; Liu, X.; Huang, Y.; Zhang, Y.; Nguyen, T.-Q.; Aramaki, S.; Bazan, G. C. *J. Am. Chem. Soc.* **2014**, *136*, 12576. (c) Puodziukynaite, E.; Wang, H.- W.; Lawrence, J.; Wise, A. J.; Russell, T. P.; Barnes, M. D.; Emrick, T. *J. Am. Chem. Soc.* **2014**, *136*, 11043. (d) Li, W.; Albrecht, S.; Yang, L.; Roland, S.; Tumbleston, J. R.; McAfee, T.; Yan, L.; Kelly, M. A.; Ade, H.; Neher, D.; You, W. *J. Am. Chem. Soc.* **2014**, *136*, 15566. (e) Liao, S.-H.; Jhuo, H.-J.; Cheng, Y.-S.; Chen, S.-A. *Adv. Mater.* **2013**, *25*, 4766.

(5) (a) He, Z.; Zhong, C.; Huang, X.; Wong, W.-Y.; Wu, H.; Chen, L.; Su, S.; Cao, Y. *Adv. Mater.* **2011**, *23*, 4636. (b) Liao, S.-H.; Li, Y.-L.; Jen, T.-H.; Cheng, Y.-S.; Chen, S.-A. *J. Am. Chem. Soc.* **2012**, *134*, 14271. (c) Seo, J. H.; Gutacker, A.; Sun, Y.; Wu, H.; Huang, F.; Cao, Y.; Scherf, U.; Heeger, A. J.; Bazan, G. C. *J. Am. Chem. Soc.* **2011**, *133*, 8416.

(6) Zhou, Y.; Fuentes-Hernandez, C.; Shim, J.; Meyer, J.; Giordano, A. J.; Li, H.; Winget, P.; Papadopoulos, T.; Cheun, H.; Kim, J.; Fenoll, M.; Dindar, A.; Haske, W.; Najafabadi, E.; Khan, T. M.; Sojoudi, H.; Barlow, S.; Graham, S.; Brédas, J.-L.; Marder, S. R.; Kahn, A.; Kippelen, B. *Science* **2012**, *336*, 327.

(7) Li, C.-Z.; Chang, C.-Y.; Zang, Y.; Ju, H.-X.; Chueh, C.-C.; Liang, P.-W.; Cho, N.; Ginger, D. S.; Jen, A. K.-Y. *Adv. Mater.* **2014**, *26*, 6262.

(8) (a) Zhang, Z.-G.; Qi, B.; Jin, Z.; Chi, D.; Qi, Z.; Li, Y.; Wang, J. *Energy Environ. Sci.* **2014**, *7*, 1966. (b) Liu, S.; Zhang, K.; Lu, J.; Zhang, J.; Yip, H.-L.; Huang, F.; Cao, Y. *J. Am. Chem. Soc.* **2013**, *135*, 15326.

(9) Dong, H.; Zhu, H.; Meng, Q.; Gong, X.; Hu, W. *Chem. Soc. Rev.* **2012**, *41*, 1754.

(10) Brédas, J.-L.; Norton, J. E.; Cornil, J.; Coropceanu, V. *Acc. Chem. Res.* **2009**, *42*, 1691.

(11) Rehm, J. M.; McLendon, G. L.; Nagasawa, Y.; Yoshihara, K.; Moser, J.; Grätzel, M. *J. Phys. Chem.* **1996**, *100*, 9577.

(12) (a) Sofos, M.; Goldberger, J.; Stone, D. A.; Allen, J. E.; Ma, Q.; Herman, D. J.; Tsai, W.-W.; Lauhon, L. J.; Stupp, S. I. *Nat. Mater.* **2009**, *8*, 68. (b) Beek, W. J. E.; Wienk, M. M.; Janssen, R. A. J. *Adv. Funct. Mater.* **2006**, *16*, 1112.

(13) Xie, Z.; Stepanenko, V.; Fimmel, B.; Würthner, F. *Mater. Horiz.* **2014**, *1*, 355.

(14) Sun, Y.; Seo, J. H.; Takacs, C. J.; Seifter, J.; Heeger, A. J. *Adv. Mater.* **2011**, *23*, 1679.

(15) Tao, T.; Lei, Y.-H.; Peng, Y.-X.; Wang, Y.; Huang, W.; Chen, Z.-X.; You, X.-Z. *Cryst. Growth Des.* **2012**, *12*, 4580.

(16) You, J.; Chen, C.-C.; Dou, L.; Murase, S.; Duan, H.-S.; Hawks, S. A.; Xu, T.; Son, H. J.; Yu, L.; Li, G.; Yang, Y. *Adv. Mater.* **2012**, *24*, 5267.

(17) (a) Jo, S. B.; Lee, J. H.; Sim, M.; Kim, M.; Park, J. H.; Choi, Y. S.; Kim, Y.; Ihn, S.-H.; Cho, K. *Adv. Energy Mater.* **2011**, *1*, 690. (b) Liu, J.; Wu, J.; Shao, S.; Deng, Y.; Meng, B.; Xie, Z.; Geng, Y.; Wang, L.; Zhang, F. *ACS Appl. Mater. Interfaces* **2014**, *6*, 8237.

(18) Cho, N.; Li, C.-Z.; Yip, H.-L.; Jen, A. K.-Y. *Energy Environ. Sci.* **2014**, *7*, 638.



DOI: 10.1021/jacs.5b02168
*J. Am. Chem. Soc.* 2015, 137, 6995−6998